

# TUNED INFRARED EMISSION FROM LITHOGRAPHICALLY-DEFINED SILICON SURFACE STRUCTURES

James T. Daly, Edward A. Johnson, William A. Stevenson, Anton C. Greenwald, John A. Wollam, Ion Optics, Inc., Waltham, MA 02452,  
Thomas George and Eric W. Jones, Jet Propulsion Laboratory, Pasadena, CA 91109

## ABSTRACT

Photonic bandgap structures have received much attention as optical and infrared filters with controllable narrow-band absorbance. There is a need, however, for the same kind of control of the thermal emittance of surfaces for applications ranging from control of radiative heat transfer to gas absorption spectroscopy. We report on the fabrication of photonic bandgap structures on silicon surfaces using standard lithographic techniques. Substrate resistivity varied from  $n^-$  to  $n^+$  and in some cases background surface emissivity was suppressed with a high reflectivity coating such as aluminum. We have measured the infrared reflectance and emittance of these patterned surfaces. Peak absorption wavelength and spectral purity (linewidth) correlate with photonic bandgap feature size and spacing as well as surface conductivity. We demonstrate band emission with a sharp short wavelength cut-off from these structures when heated.

## INTRODUCTION

The optical properties of periodic dielectric arrays have attracted recent interest. [1,2] When electromagnetic waves with wavelength on the order of the period of the dielectric array propagate through this structure, the light interacts in a manner analogous to that for electrons in a periodic symmetric array of atoms. The structure exhibits allowed and forbidden extended states, a reciprocal lattice, Brillouin zones, Bloch wavefunctions, etc. [3,4,5] These "photonic bandgap" structures, or photonic crystals, have been developed as transmission/reflection filters, low-loss light-bending waveguides, and for inhibiting spontaneous emission of light in semiconductors which could lead to zero-threshold diode lasers [6].

Metal grid structures are recognized as spectrally selective filters at microwave, millimeter and far infrared wavelengths [7,8,9] One such set of structures is depicted in figure 1, which shows metal mesh and crossed dipole structures. The important result is that the transmission curves exhibit a relatively narrow bandpass which is related to feature size.

Ion Optics currently manufactures and distributes the *pulsIR*<sup>®</sup> infrared radiator (figure 2). Emissivity of these metal filaments is controlled by creating random surface texture (sub-micron scale rods and cones) which modifies the surface absorption spectrum. For wavelengths small compared to the feature sizes, the surface scatters incoming light and has high emissivity (>80%) – the filaments appear visibly black. For wavelengths long compared to the feature sizes, the surface has low emissivity, characteristic of a flat metal (<0.1). The measured emission spectrum (Figure 2) illustrates the operating principle of the device – the emission spectrum is just the Planck function modulated by the absorption spectrum of the filament surface. [10,11] We can control the wavelength of the transition edge between high and low emissivity by controlling average feature size and depth (height.) By suppressing emission at long wavelengths, we force the filament to reach thermal equilibrium with its drive pulse at a higher temperature. This, in turn, pulls the blackbody curve to shorter wavelengths and produces enhanced emission at

wavelengths shorter than the cut-off wavelength. The resulting emission band is fairly broad, and in this work, we attempt to narrow the emission width by enforcing a short wavelength cut-off.

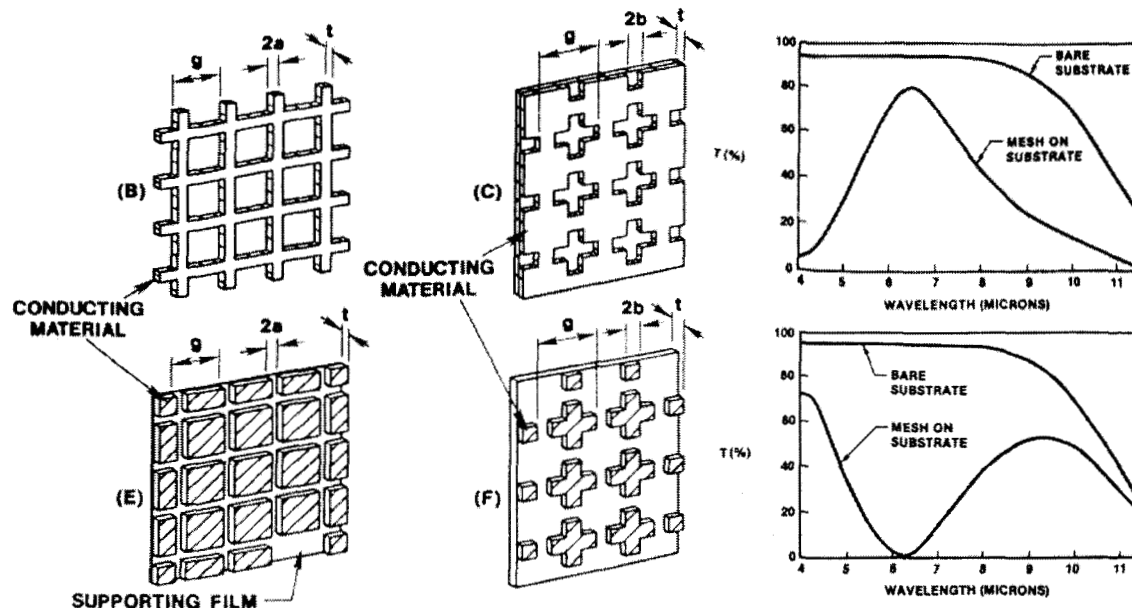


**Figure 1** Inductive (b,c) and capacitive (e,f) metal mesh filters (micro-antenna arrays) and their respective spectral transmission [8].

Our goal then was to develop an infrared thermal emitter with high emissivity over a narrow band of wavelengths ( $D/\lambda \sim 0.1$ ) and low emissivity everywhere else. Such sources, emitting hundreds of milliwatts of power in-band, are attractive alternatives to infrared light emitting diodes (IRLEDs) which have low quantum efficiencies ( $\sim 2-4\%$ ) and only tens of microwatts output power. We chose to make the tuned emitters by making non-random patterns, periodic arrays similar to metal mesh and photonic bandgap filters, on the emitter's surface. Since we needed wavelengths in the range 2-14  $\mu\text{m}$  for spectroscopy, this implies sizes as small as 0.5  $\mu\text{m}$  which are readily fabricated by lithography on silicon. To our knowledge, this is the first report of photonic bandgap structures as tuned thermal emitters. **In particular, we find the peak emission wavelength is proportional to the spacing of the lithographic pattern.**

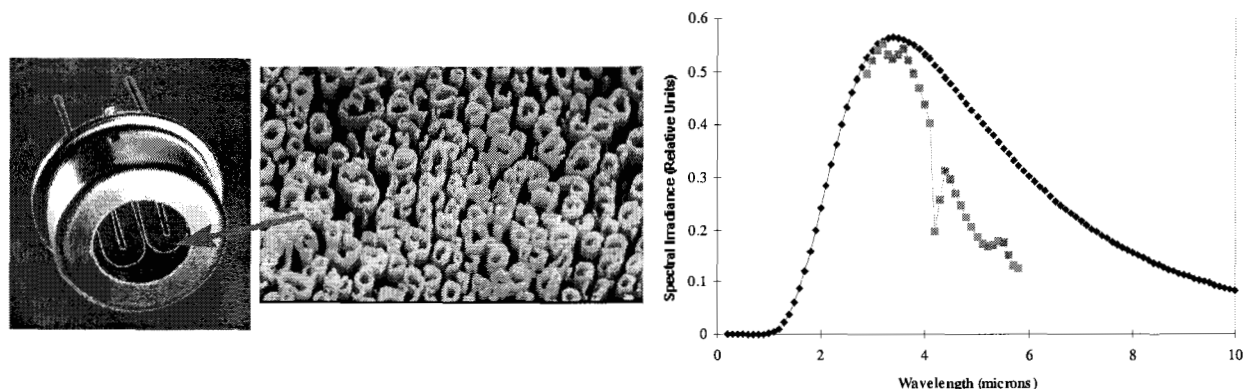


**Figure 2** Ion Optics current TO-8 sized pulsIR<sup>®</sup> product, SEM micrograph of surface texture, and grating monochromator scan of thermal emission (compared to Planck radiation) shows the long wavelength emissivity cut-off achieved by random texture.

## EXPERIMENTAL

We selected patterns based on the previous work of Byrne, *et al.* [8,9] because of the relatively simple relation given and demonstrated between feature size and transmission wavelength. Specifically, we used the crossed dipole pattern depicted in figure 1 and fabricated a variety of feature sizes and spacings. A summary of the patterns used is given in table 1 and Figure 3.

**Table 1** Summary of crossed dipole patterns etched into silicon wafers.

pattern designation	cross length, L (mm)	line width, 2b (mm)	Center-to-center spacing, g (mm)
8B	4.0	1.7	5.0
10B	5.0	1.9	6.0
12B	6.0	2.2	7.1
8N	3.8	1.0	6.4
10N	4.8	1.2	8.0
12N	5.7	1.4	9.5
5.25N	2.5	0.6	4.2
3.4N	1.6	0.4	2.7

Photomasks, made by direct write e-beam lithography, were purchased from Dupont. Lithography and etching was performed at the Microdevices Laboratory at JPL. The basic fabrication sequence was: deposit photoresist; expose pattern on resist; reactive ion etch (RIE) for 5, 10 or 15 minutes to form the cross-shaped cavities of different depths with straight side-walls; and remove photoresist. Five  $n^-$  and two  $n^+$  wafers were processed. One  $n^-$  and one  $n^+$  wafer were coated with 500A chromium (for adhesion) followed by 1000A gold before lifting-off with removal of the photoresist, leaving gold coating at the bottom of the etched cavities. In another case, an  $n^-$  wafer was coated with aluminum to suppress the background emissivity. In this case, metal covered the unetched regions as well as the bottom of the cavities.

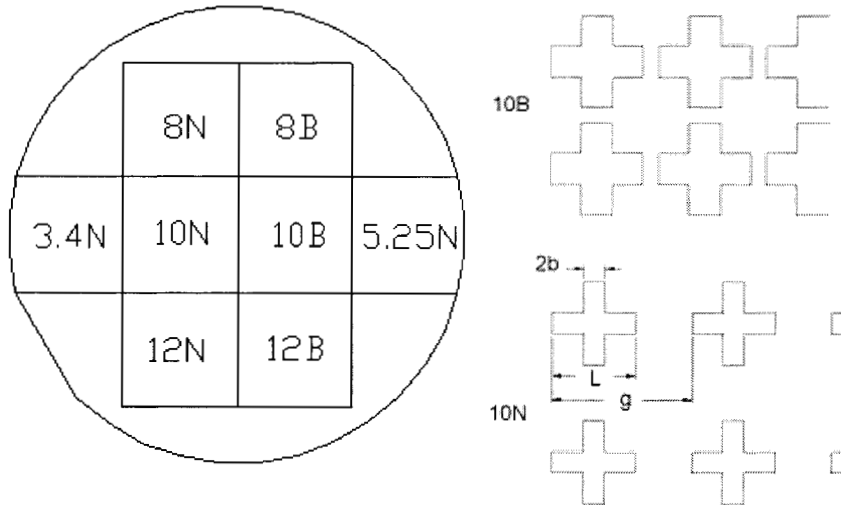


**Figure 3** Mask pattern for whole 3 inch diameter wafer on left showing regions designed for reflecting 8, 10, and 12 micron IR etc. Design detail on right for broad (B, top) and narrow (N, bottom) line features.

Scanning electron microscopy (SEM) was used to confirm etched cavity depth and to verify that the side-walls were straight. Reflectance spectra were measured at room temperature over the range 2.5–25 nm using a MIDAC FTIR spectrometer ( $0.5\text{ cm}^{-1}$  resolution) with a surface reflectance attachment that set the angle of incidence at 45 degrees. Thermal emittance measurements and additional room temperature reflectance measurements at near normal incidence were made over the range 3–11 nm using a chalcogenide fiber-coupled MIDAC FTIR spectrometer with MCT detector ( $0.4\text{ cm}^{-1}$  resolution). During the emittance measurements, samples were placed on a hot plate or heated sample stage covered with a thin ( $\sim 1\text{ mm}$ ) graphite sheet and confirmed to be at 300 C, 400 C, or 500 C with a type K thermocouple.

## RESULTS

SEM measurements, shown in figure 4, confirm that the etch depth was about 2.2 nm for samples etched 5 min, about 6.2 nm for samples etched 10 min, and about 9.4 nm for samples etched for 15 min. Actual depths varied  $\pm 5\%$  depending on the width of the structure. For example, features with the “N” designation (for narrow line width) were generally etched to lesser depths than those designated “B” (for broad line width).

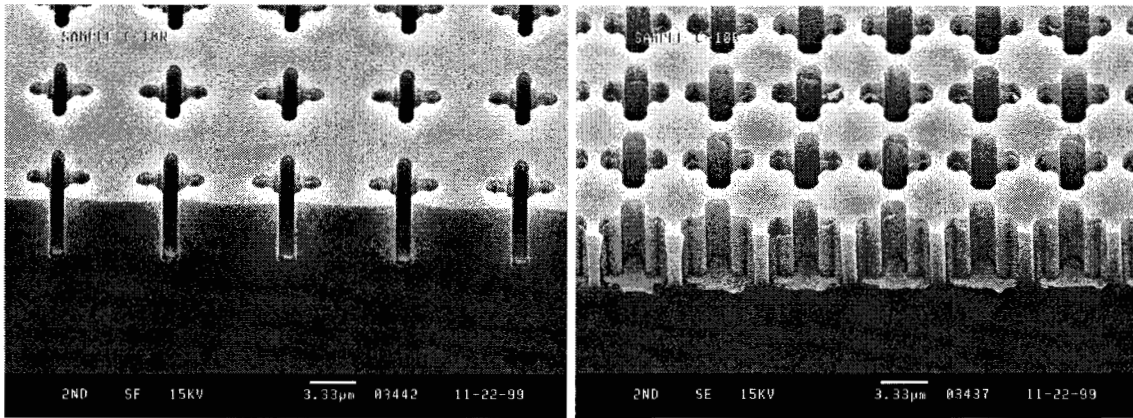


**Figure 4** SEM photos of patterns 10N and 10B. This confirms the depth as  $6.0\text{ }\mu\text{m}$  and  $6.3\text{ }\mu\text{m}$ , respectively, and the presence of Cr/Au metallization at the bottom of the cavity. The photo also shows rounding of the sharp corners of the pattern.

Room temperature reflectance measurements showed the uncoated wafers to have a nominal 30%-40% reflectance typical of bare silicon except in a range which exhibited narrow band absorbance peaks as shown in figure 5. The absorbance peaks are relatively narrow and occur at longer wavelengths for larger feature sizes. Unlike the  $n^-$  and aluminum-coated  $n^-$  wafers, the  $n^+$  wafers did not show any unusual absorbance peaks.

Thermal emittance measurements showed enhanced emissivity for wavelengths in the range 5 – 10 nm depending upon feature size. For features with narrow line width (labeled “N”), the enhancement is slight, but for the larger features (labeled “B”), the enhancement is significant. Figure 6 shows the emittance data for sample F at 500C. The relation between feature size and emittance peak is striking and is further illustrated in Figure 7.

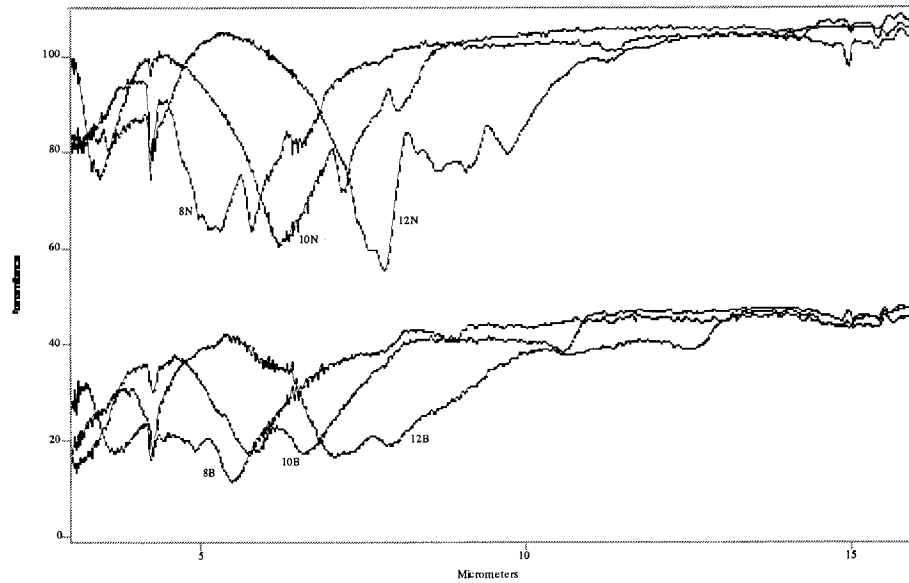


**Figure 5** Reflectance of aluminum-coated  $n^-$  silicon. For narrow linewidth features, reflectance is high (like aluminum) with narrow absorbance peaks. For broader linewidths, reflectance is reduced but still exhibits absorbance peaks. In both cases, the position of the peak is related to feature size.

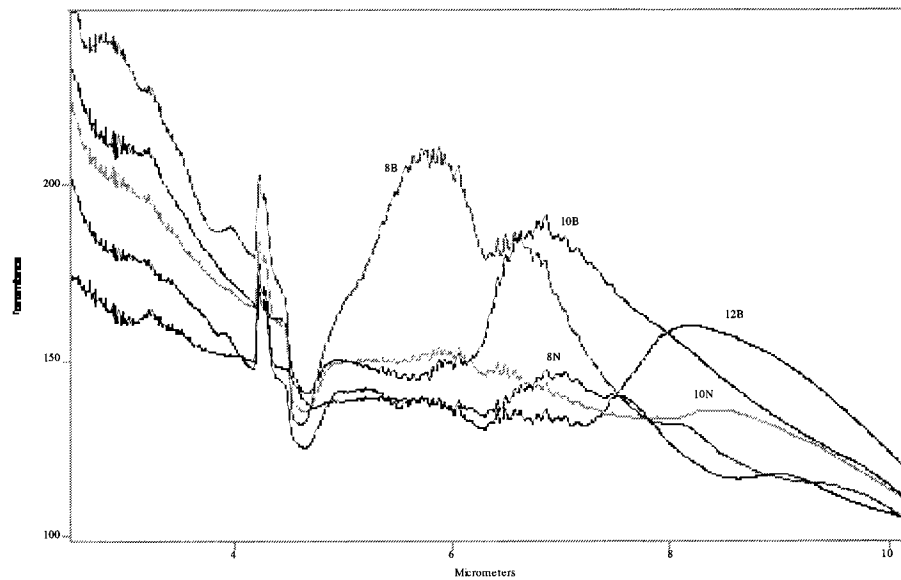


**Figure 6** Thermal emittance at 500°C for aluminum-coated  $n^-$  silicon. The narrow linewidth features exhibit weak peaks while the broad linewidth features exhibit strong peaks. Again, both show a wavelength dependence related to feature size.

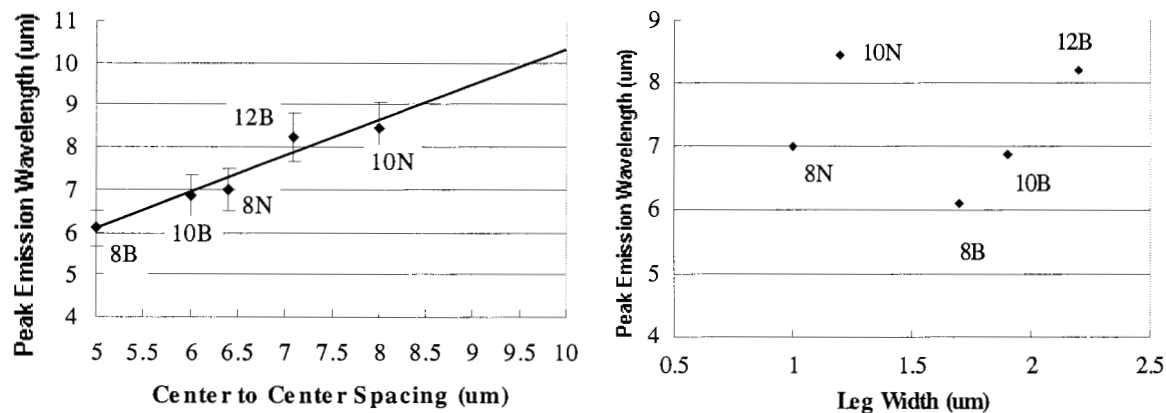


**Figure 7** Relationship between peak thermal emittance wavelength and (a) feature spacing and (b) feature linewidth.

## CONCLUSIONS

This work has showed that lithographically defined surface structures can produce distinct emission bands, clearly related to feature size, when heated. These emission bands observed from n- wafers, with and without aluminum overcoating, are absent from n+ wafers with similar surface structures. They correspond to absorption bands in reflection spectra from the same surfaces. The short-wavelength shoulders of these peaks are sharp, consistent with a half-width approximately equal to  $1/6$ . This half-width is comparable to infrared light emitting diodes (LEDs), but the energy in the peak band is orders of magnitude larger. This offers promise for a new class of tunable infrared emitter devices.

## ACKNOWLEDGEMENTS

This work is supported in part by the National Science Foundation under grant no. DMI-9860975, by a NIST Advanced Technology Program contract no: ATP-99-01-2051. The research performed at the Center for Space Microelectronics Technology, Jet Propulsion Laboratory, California Institute of Technology was sponsored by the National Aeronautics and Space Administration, Office of Space Science. The authors thank Ramesh Patel and Dave Chin for help with sample preparation and reflectance measurements.

## REFERENCES

- 1 See for example, the special issue of *J. Mod Opt.*, **41**, 173 (1994).
- 2 See the special issue of *J. Opt. Am. B*, **10**, 208 (1993).
- 3 E. Yablonovitch and T.J. Gmitter, *Phys. Rev. Lett.*, **63**, 1950 (1989).
- 4 E. Yablonovitch and T.J. Gmitter, *Phys. Rev. Lett.*, **67**, 3380 (1991).
- 5 E. Yablonovitch, *J. Phys.: Condens. Matter*, **5**, 2443 (1993).
- 6 E. Yablonovitch, *Phys. Rev. Lett.*, **58**, 2059 (1987).
- 7 S.T. Chase and R.D. Joseph, *Appl. Optics*, **22**, 1775 (1983).
- 8 D.M. Byrne, A.J. Brouns, F.C. Case, R.C. Tiberio, B.L. Whitehead, and E.D. Wolf, *J. Vac. Sci. Technol. B* **3**, 268 (1985).
- 9 D.M. Byrne, *Proc. SPIE*, **560**, 70 (1985).
- 10 Ed Johnson, US patent 5,838,016, 1998.
- 11 C. C. Blatchley, E.A Johnson, Y.-K. Pu, C. Von Benken, *Proc. SPIE*, **1753**, 317 (1992).